

# Oxide systems – an answer to the qubit problem?

Sudhakar Yarlagadda  
Saha Institute of Nuclear Physics  
Kolkata

Collaborators: Amit Dey & M. Q. Lone

8/Dec./2015

- Last few decades witnessed incredible success of semiconductor devices.
- Now at the midst of a similar revolution based on oxide materials.
- Diverse phenomena in oxides (such as magnetism, superconductivity, etc.) are finding applications in data storage, fast-transistors, etc.
- Potential of oxides as device materials is only beginning to be explored.
- Low-dimensional oxides present new opportunity where electronic and magnetic properties can be optimized by engineering many-body interactions, geometries, fields, strain, disorder, etc.
- Need to exploit new physics and develop new devices to meet challenges such as miniaturization, decoherence-free and dissipationless operations, etc.

# comparison between semiconductors and oxides

<u>Semiconductors</u>	<u>Oxides</u>
<b>Physics:</b> <ul style="list-style-type: none"><li>▶ large overlap of s/p orbitals gives extended wavefunctions.</li><li>▶ no intrinsic magnetism or other correlations.</li></ul>	<b>Physics:</b> <ul style="list-style-type: none"><li>▶ localization of 3d/2p orbitals give strong Coulomb interaction.</li><li>▶ diverse magnetic, charge, orbital correlations.</li></ul>
<b>Technology:</b> <ul style="list-style-type: none"><li>▶ Quality: high! can be fabricated into complex structures.</li><li>▶ Understanding: Semiconductor modelling is straightforward.</li><li>▶ Tunability: control charge with modest doping/ E fields.</li></ul>	<b>Technology:</b> <ul style="list-style-type: none"><li>▶ Quality: materials chemistry challenging; fabrication less developed.</li><li>▶ Understanding: strong correlations challenging to theoretical tools.</li><li>▶ Tunability: high! due to competing ordered states.</li></ul>

vastly richer physics suggests entirely new functionalities provided  
**The Oxides Grand Challenge** can be met :

To achieve the same level of synthetic control and fundamental understanding as is currently attained in semiconductors and simple metals.

## Phase Diagram (Cheong *et al.*):

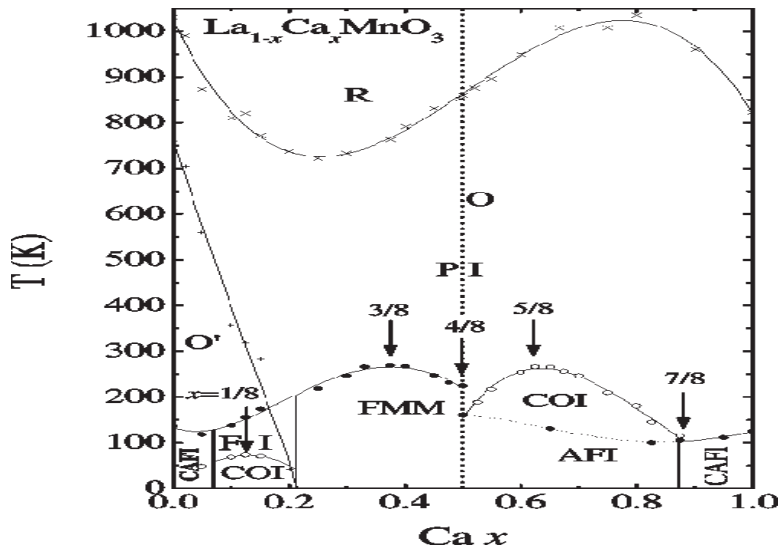
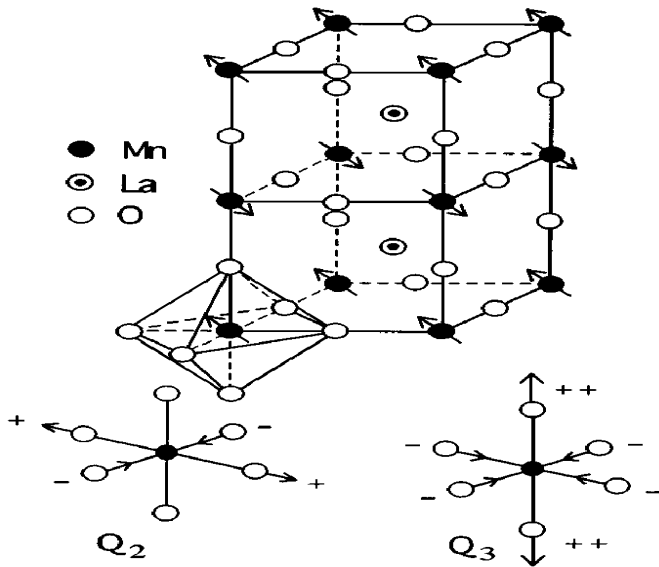
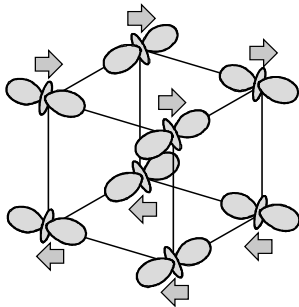


Figure: Exotic orbital, charge, and spin ordering in  $\text{La}_{1-x}\text{Ca}_x\text{MnO}_3$

# $\text{LaMnO}_3$ Structure (Edwards):



## Orbital order in $LaMnO_3$ (Maekawa):



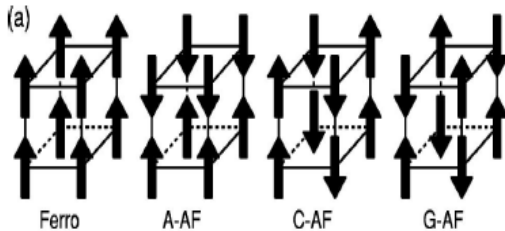


Figure: A-AF corresponds to  $LaMnO_3$  while G-AF to  $SrMnO_3$  or  $LaFeO_3$  (Dagotto)

# Our work outline

- ▶ Introduction:  
Charge qubit from electron in tunnel-coupled double quantum dot (DQD). Quantum dots from oxides a new area of research. Oxides good candidates for miniaturization and coherence
- ▶ Two spin interacting system locally coupled to optical phonons
- ▶ Decoherence analysis using non-Markovian master equation
- ▶ Markovian dynamics for Infinite-range Heisenberg model
- ▶ Quantum control of decoherence using dynamic decoupling
- ▶ Summary and conclusions

- ▶ Quantum computing is a current major challenge; expected to solve fast many complex problems.
- ▶ Quantum bit (qubit) is building block of quantum computer.
- ▶ Superposition principle distinguishes a quantum bit (qubit) from a classical bit.
- ▶ Interference of two states of a bit (like interference in waves) that lends quantumness to qubit.
- ▶ Interaction of qubits with environmental noise is inevitable; coupling to noise degrades superposition of states in qubit, i.e., produces decoherence.
- ▶ We show that charge qubit, realized in oxide-based double quantum dot (DQD), has very small decoherence and size of the system can be only a few nanometers.
- ▶ Usual charge qubit based on semiconductor DQD decoheres significantly (in less than 10 ns) and size is an order of magnitude larger.

- ▶ Our charge qubit, an electron tunneling between two oxide dots, maintains coherence provided system and environment (comprising of optical phonons) are initially uncorrelated in frame of reference where electron is dressed by deformation it produces in lattice environment.
- ▶ We show that stronger the electron couples to environment the lesser is qubit decoherence.
- ▶ Substantial experimental evidence for strong electron-phonon interaction in manganites (EXAFS).
- ▶ Coherence protected due to energy of environmental optical phonons (produced by the relative vibrations of atoms at each site) is much larger than excitation energy of DQD; thus, no exchange of energy takes place between electron and environment.
- ▶ Stronger noise protects quantumness in a qubit!

## Double quantum dot

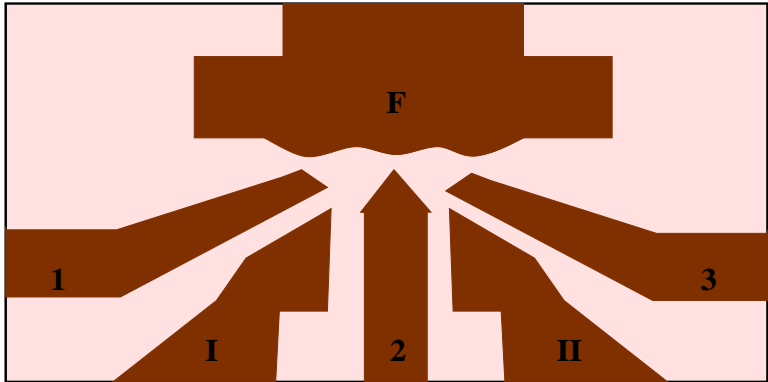


**Figure:** Schematic of a double quantum dot defined by metallic gates (dark areas).

# Interacting two spin system with equal site-energies

Anisotropic Heisenberg interaction:

$$H_s = J_{\parallel} S_1^z S_2^z - \frac{J_{\perp}}{2} (S_1^+ S_2^- + S_2^+ S_1^-).$$

Local phonon Hamiltonian:

$$H_{env} = \sum_{k;i=1,2} \omega_k a_{k,i}^{\dagger} a_{k,i}.$$

Spin-phonon local interaction (strong coupling  $g > 1$ ):

$$H_I = \sum_{k;i=1,2} g_k \omega_k S_i^z (a_{k,i} + a_{k,i}^{\dagger}).$$

Initially consider only one k-mode. Lang-Firsov transformation:

$$H_{LF} = e^S H e^{-S}$$

$S = -\sum_i g S_i^z (a_i - a_i^{\dagger}) \rightarrow$  Transformation generator.

$$H_s^{LF} = J_{\parallel} S_1^z S_2^z - \frac{J_{\perp} e^{-g^2}}{2} (S_1^+ S_2^- + S_2^+ S_1^-)$$

⇒ spins coupled to the mean phonon field and with reduced hopping amplitude due to formation of polaron. Harmonic oscillators are displaced.

$$H_{env}^{LF} = \sum_{i=1,2} \omega a_i^{\dagger} a_i.$$

$$H_i^{LF} = -\frac{1}{2} [J_{\perp}^+ S_1^+ S_2^- + J_{\perp}^- S_2^+ S_1^-]$$

⇒ Spins coupled to local phonon fluctuations around mean field. This contains uncontrolled degrees of freedom.

$$J_{\perp}^{\pm} = J_{\perp} e^{\pm g[(a_2 - a_2^{\dagger}) - (a_1 - a_1^{\dagger})]} - J_{\perp} e^{-g^2}$$

$$\langle J_{\perp} e^{\pm g[(a_2 - a_2^{\dagger}) - (a_1 - a_1^{\dagger})]} \rangle_{T=0} = J_{\perp} e^{-g^2}$$

The two  $S_T^z = 0$  eigenstates are :

$$|\varepsilon_t\rangle = \frac{1}{\sqrt{2}}(|\uparrow\downarrow\rangle + |\downarrow\uparrow\rangle)$$

and

$$|\varepsilon_s\rangle = \frac{1}{\sqrt{2}}(|\uparrow\downarrow\rangle - |\downarrow\uparrow\rangle).$$

$S_T^z = 0$  subspace is a decoherence free subspace [DFS] for spins coupled to global phonons

So, the energy gap is much smaller than the phonon energy in the strong coupling ( $g^2 \gg 1$ ) and non-adiabatic ( $\frac{J_{\perp}}{\omega} \leq 1$ ) limit:

$$J_{\perp} e^{-g^2} \ll \omega.$$

PHYSICAL REVIEW B 89, 064311 (2014), A. Dey and Sudhakar Yarlagadda.

# Decoherence analysis using non-Markovian master equation

Using time convolutionless (TCL) projection operator technique the non-Markovian master equation up to second order in perturbation is given by

$$\frac{d\tilde{\rho}_s(t)}{dt} = - \int_0^t d\tau \text{Tr}_R[\tilde{H}_I(t), [\tilde{H}_I(\tau), \tilde{\rho}_s(t) \otimes R_0]].$$

where  $\tilde{\rho}_s(t) \equiv \text{Tr}_R[\tilde{\rho}_T(t)]$

Assume initially  $\rho_T(0) = \rho_s(0) \otimes R_0$ .

Initial Bath state:  $R_0 = \sum_n \frac{e^{-\beta\omega_n}}{Z} |n\rangle_{ph} \langle n|$ .

Interaction picture:  $\tilde{H}_I(t) = e^{iH_0 t} H_I e^{-iH_0 t}$  and  
 $\tilde{\rho}_T(t) = e^{iH_0 t} \rho_T(t) e^{-iH_0 t}$

where  $H_0 = H_s + H_{env}$

## Preparation of separable initial state $\rho_T(0) = \rho_s(0) \otimes R_0$

Start with gate voltage set to  $J_{\perp} = 0$  and introduce an electron in one of the quantum dots to obtain the state

$$|10\rangle \otimes |0\rangle_{ph} \propto (|\varepsilon_s\rangle + |\varepsilon_t\rangle) \otimes |0\rangle_{ph}.$$

Introduce small tunneling  $J_{\perp}/\omega \ll 1$  (say  $10^{-3}$ ) rapidly and let the system evolve.

For small  $J_{\perp}/\omega$ ,  $|\varepsilon_s\rangle \otimes |0\rangle_{ph}$  and  $|\varepsilon_t\rangle \otimes |0\rangle_{ph}$  are approximate eigenstates (of the Hamiltonian in the LF frame) with probability larger than  $1 - J_{\perp}^2/(g^4\omega^2)$  (i.e.,  $> 0.999999$ ).

The evolved state is a general separable initial state (in the **dressed basis**) given by:

$$|\psi(t)\rangle \propto [\cos(J_{\perp} e^{-g^2} t/2)|10\rangle + ie^{-i\phi} \sin(J_{\perp} e^{-g^2} t/2)|01\rangle] \otimes |0, 0\rangle_{ph}$$

where  $e^{i\phi}$  is Aharnov-Bohm phase factor due to a magnetic flux.

Change the gate voltage and the magnetic flux rapidly to get the desired value of tunneling  $J_{\perp}$ .

For large coupling strength ( $g^2 \gg 1$ ), the long time values of the matrix elements are estimated as:

$$\begin{aligned} \left. |\langle \varepsilon_s | \rho_s(t) | \varepsilon_t \rangle| \right|_{t \rightarrow \infty} &= |\langle \varepsilon_s | \rho_s(0) | \varepsilon_t \rangle| \exp \left[ -\frac{1}{4g^2} \left( \frac{J_{\perp}}{g\omega} \right)^2 \right] \\ \left. \langle \varepsilon_s | \rho_s(t) | \varepsilon_s \rangle \right|_{t \rightarrow \infty} &= \frac{1}{2} \langle \varepsilon_s | \rho_s(0) | \varepsilon_s \rangle \left\{ 1 + \exp \left[ -\frac{1}{8g^2} \left( \frac{J_{\perp}}{g\omega} \right)^2 \right] \right\} \\ &\quad + \frac{1}{2} \langle \varepsilon_t | \rho_s(0) | \varepsilon_t \rangle \left\{ 1 - \exp \left[ -\frac{1}{8g^2} \left( \frac{J_{\perp}}{g\omega} \right)^2 \right] \right\} \end{aligned}$$

Here, the initial density matrix  $\rho_s(0)$  is considered to be real.  
The coherence factor:

$$C(t) = \frac{|\langle \varepsilon_s | \rho_s(t) | \varepsilon_t \rangle|}{|\langle \varepsilon_s | \rho_s(0) | \varepsilon_t \rangle|}$$

Inelastic factor (indicating dissipation) or population difference:

$$P(t) = \frac{\langle \varepsilon_s | \rho_s(t) | \varepsilon_s \rangle - \langle \varepsilon_t | \rho_s(t) | \varepsilon_t \rangle}{\langle \varepsilon_s | \rho_s(0) | \varepsilon_s \rangle - \langle \varepsilon_t | \rho_s(0) | \varepsilon_t \rangle}$$

# Plots:

coherence factor:

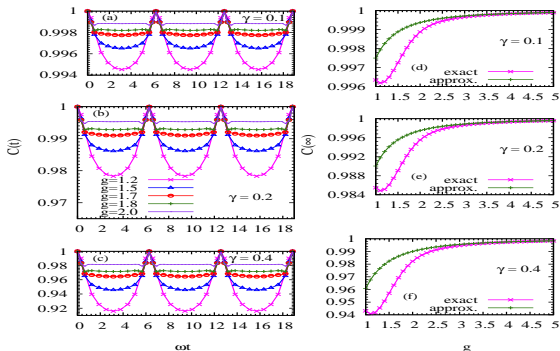


Figure:  $\gamma = \frac{J_{\perp}}{g\omega}$ . For large values of  $g$ ,  $C(\infty)$  match with the  $C(t)$  values between  $2n\pi$  and  $2(n+1)\pi$  values of  $\omega t$ .

# Finite-temperature decoherence for $kT \sim \omega$

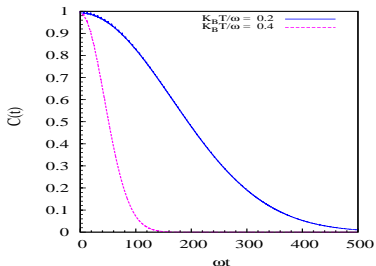
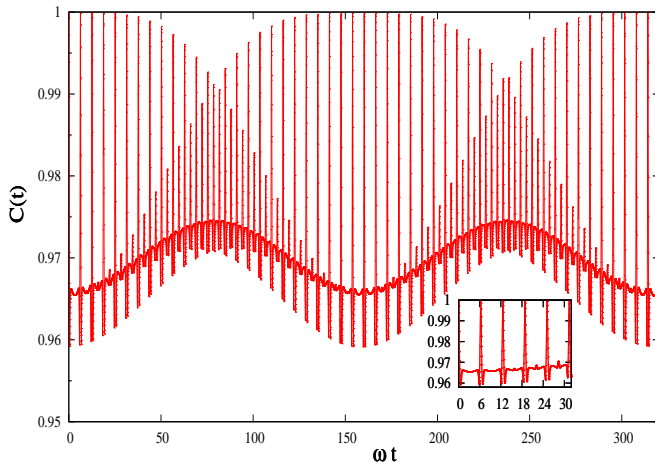


Figure: Coherence dynamics for  $g = 2$ ,  $\frac{J_{\perp}}{\omega} = 0.5$  and  $\Delta\varepsilon = 0.0$ .

$$\begin{aligned} & \sum_m \int_0^t d\tau \text{ }_{ph} \langle n | J_{\perp}^+(t) | m \rangle_{ph} \text{ }_{ph} \langle m | J_{\perp}^-(\tau) | n \rangle_{ph} \frac{e^{-\beta\omega_n}}{Z} \\ &= \sum_m \frac{e^{i(\omega_n - \omega_m)t} - 1}{i(\omega_n - \omega_m)} \langle n | J_{\perp}^+ | m \rangle_{ph} \text{ }_{ph} \langle m | J_{\perp}^- | n \rangle_{ph} \frac{e^{-\beta\omega_n}}{Z} \end{aligned}$$

Including the effect of small  $J_{\perp} e^{-g^2}/\omega$ :



**Figure:**  $J_{\perp} e^{-g^2}/\omega = 0.02$  and  $g = 2$ . Inset shows that  $C(t)$ , for  $\omega t/2\pi \sim 1$ , is similar to case when  $J_{\perp} e^{-g^2}$  is ignored compared to  $\omega$ .

Including large number of bath modes ( $0.9\omega_u \leq \omega_k \leq \omega_u$ ):

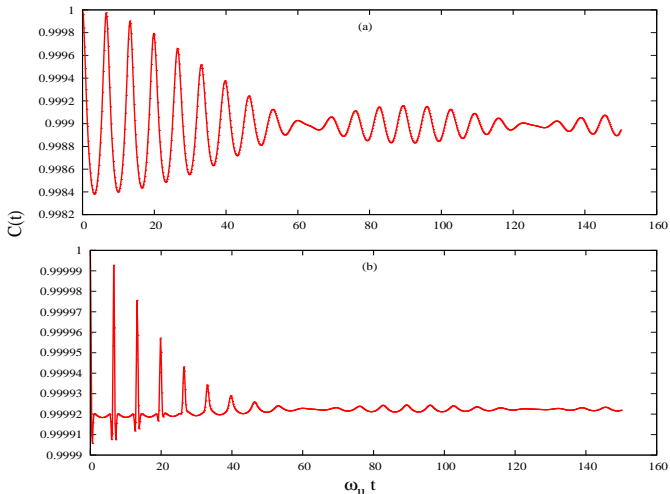


Figure: (a)  $J_{\perp}/\omega_u = 0.05$  and  $\frac{\sum_k g_k^2}{N} = 1$ ; (b)  $J_{\perp}/\omega_u = 0.05$  and  $\frac{\sum_k g_k^2}{N} = 4$ .

Inelasticity (dissipation):

Decoherence and dissipation are less for smaller  $\gamma$  and larger  $g$  values.

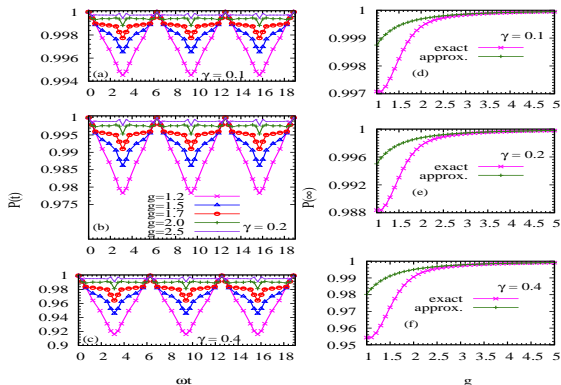


Figure:  $\gamma = \frac{J_{\perp}}{g\omega}$ . For large values of  $g$ ,  $P(\infty)$  match with  $P(t)$  at  $\omega t$  values between two consecutive multiples of  $\pi$ .

## Two-site HCB model with different site energies

$$\begin{aligned} H = & \varepsilon_1(n_1 - \frac{1}{2}) + \varepsilon_2(n_2 - \frac{1}{2}) - \frac{J_{\perp}}{2}(b_1^{\dagger}b_2 + b_2^{\dagger}b_1) \\ & + J_{\parallel}(n_1 - \frac{1}{2})(n_2 - \frac{1}{2}) + g\omega \sum_{i=1,2} (n_i - \frac{1}{2})(a_i + a_i^{\dagger}) \\ & + \omega \sum_{i=1,2} a_i^{\dagger}a_i \end{aligned}$$

with strong (compared to reduced tunnelling  $J_{\perp}e^{-g^2}$ ) site energy  $\varepsilon_i$  at site  $i$

$b_i$  is the HCB destruction operator at site  $i$ .  $\{b_i, b_i^{\dagger}\} = 1$ ,  
 $[b_i, b_j^{\dagger}] = 0$  for  $i \neq j$ .

## Role of proximity of $\Delta\varepsilon$ to phonon eigenenergy:

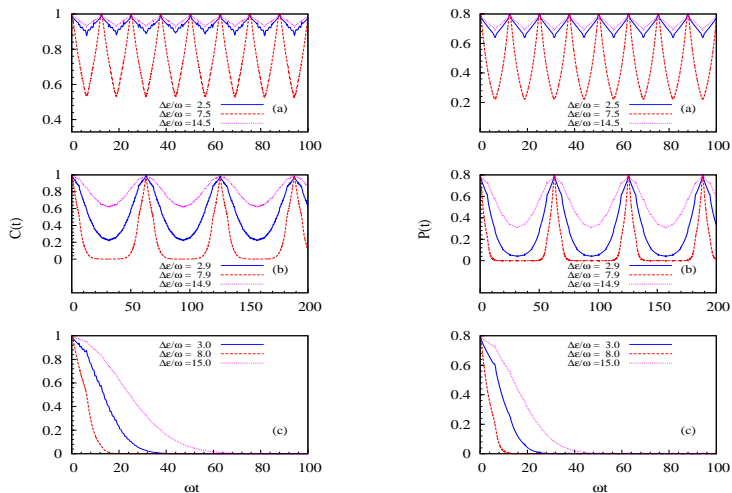


**Figure:** Time dependence of  $C(t)$  and  $P(t)$  for  $\frac{J_{\perp}}{\omega} = 1.0$ ,  $g = 2.0$ , and when (a)  $\frac{\Delta\varepsilon}{\omega} = 2.5, 7.5$  and  $14.5$ ; (b)  $\frac{\Delta\varepsilon}{\omega} = 2.9, 7.9$  and  $14.9$ ; and (c)  $\frac{\Delta\varepsilon}{\omega} = 3.0, 8.0$  and  $15.0$ ; the initial population of the excited state being  $P(0) = 0.8$ .

## Multi-mode phonons:

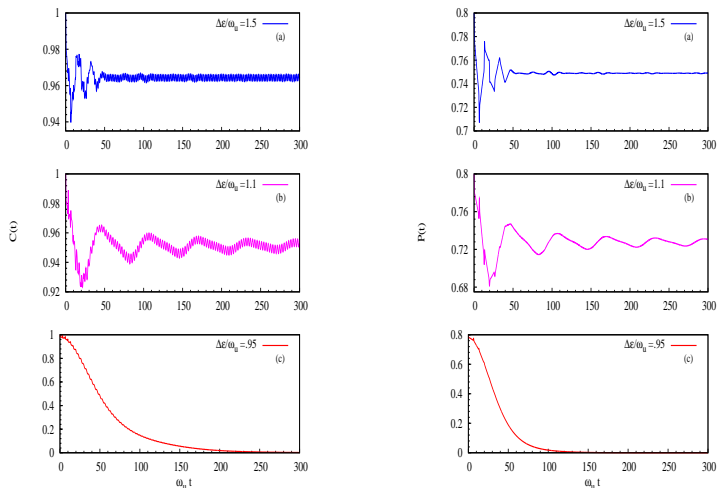


**Figure:** Time dependence of  $C(t)$  and  $P(t)$  for  $\frac{J_{\perp}}{\omega_u} = 1.0$ ,  $\frac{\omega_l}{\omega_u} = 0.9$ ,  $g = 2.0$  and different values of  $\frac{\Delta\varepsilon}{\omega_u}$ ; the initial population of the excited state being  $P(0) = 0.8$ .

Proximity of  $\Delta\varepsilon$  to twice the polaronic energy  $2g^2\omega$ :

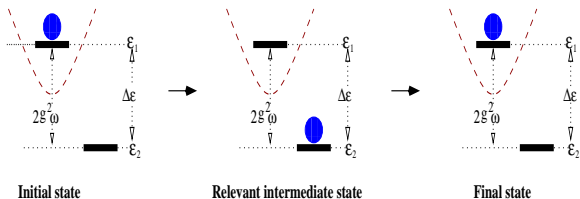


Figure: Diagrammatic presentation of the second order hopping process.

Energy difference between the initial and the intermediate states  
 $(\varepsilon_1 - g^2\omega) - (\varepsilon_2 + g^2\omega) = \Delta\varepsilon - 2g^2\omega \rightarrow 0$

$\Rightarrow$  second order hopping process becomes more dominant leading to stronger decoherence

Phys. Rev. B **92**, 094302 (2015), A. Dey, M. Q. Lone and S. Yarlagadda.

# Finite-temperature

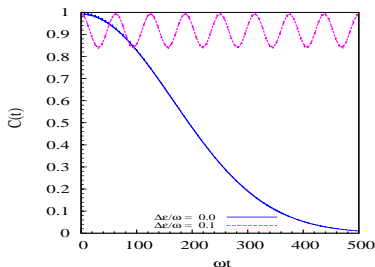


Figure: Coherence dynamics for  $g = 2$ ,  $\frac{J_{\perp}}{\omega} = 0.5$  and  $K_B T/\omega = 0.2$ .

$$\sum_m \int_0^t d\tau e^{i\Delta\epsilon(t-\tau)} {}_{ph}\langle n | J_{\perp}^+(t) | m \rangle_{ph} {}_{ph}\langle m | J_{\perp}^-(\tau) | n \rangle_{ph} \frac{e^{-\beta\omega_n}}{Z}$$

$$= \sum_m \frac{e^{i(\Delta\epsilon + \omega_n - \omega_m)t} - 1}{i(\Delta\epsilon + \omega_n - \omega_m)} {}_{ph}\langle n | J_{\perp}^+ | m \rangle_{ph} {}_{ph}\langle m | J_{\perp}^- | n \rangle_{ph} \frac{e^{-\beta\omega_n}}{Z}$$

# Infinite range HCB model

$$H_T = \sum_{i,j>i} \left[ \frac{-J_{\perp}}{2} (b_i^{\dagger} b_j + \text{H.c.}) + J_{\parallel} (n_i - \frac{1}{2})(n_j - \frac{1}{2}) \right] \\ + \omega \sum_j a_j^{\dagger} a_j + g\omega \sum_j (n_j - \frac{1}{2})(a_j + a_j^{\dagger})$$

Hopping strength independent of the distance between sites  
 $J_{\perp} > 0$ ,  $J_{\parallel} > 0$ ,  $J_{\perp} = J_{\perp}^*/(N-1)$ ,  $J_{\parallel} = J_{\parallel}^*/(N-1)$   
strong coupling  $g^2 \gg 1$  and nonadiabatic  $J_{\perp}^*/\omega \leq 1$  regime

$$H^{eff} = H_s^L + H^{(2)}$$

- has the same set of eigenstates as those of  $H_s^L \Rightarrow$  Robust eigenstates
- consequence of infinite range of the model

Phys. Rev. B **92**, 094302 (2015), A. Dey, M. Q. Lone and S. Yarlagadda.

# Markovian dynamics

$J_{\perp}^* e^{-g^2} \ll \omega \Rightarrow \tau_c \ll \tau_s \rightarrow$  justification for Markov process

$$\begin{aligned} \frac{d\tilde{\rho}_s(t)}{dt} &= -i \text{Tr}_R[\tilde{H}_I^L(t), \rho_s(0) \otimes R_0] \\ &\quad - \int_0^{\infty} d\tau \text{Tr}_R[\tilde{H}_I^L(t), [\tilde{H}_I^L(t-\tau), \tilde{\rho}_s(t) \otimes R_0]] \end{aligned}$$

Second order Markovian quantum master equation  
at  $T = 0K$  and with fixed  $\sum_i n_i$

$$\frac{d\rho_s(t)}{dt} = -i [H^{\text{eff}}, \rho_s(t)]$$

form of von Neumann equation  $\rightarrow$  governs the unitary evolution  
of reduced density matrix

${}_s\langle n | \rho_s(t) | m \rangle_s = e^{-i(E_n - E_m)t} {}_s\langle n | \rho_s(0) | m \rangle_s \Rightarrow$  **no decoherence**  
decoherence free behavior is the consequence of **long-range** of the  
model, **strong coupling**, **fixed total particle number** and  
**Markov process**.

## Summary and conclusions

- Using GaAs DQDs, Petta et al. [PRL **86**, 246804 (2010)], Ritchie et al. [Nano Letters **10**, 2789 (2010)] obtain decoherence times  $\sim 10$  ns.
- In oxide materials, dominant interaction is with optical phonons. Analyzing optical phonon environment, we get a small decoherence even for local noise [Phys. Rev. B **89**, 064311 (2014)] & [Phys. Rev. B **92**, 094302 (2015)].
- For Heisenberg interaction, fast manipulation and dynamical decoupling is possible for the spin states.
- Miniaturization demands replacement of silicon technology
- Oxides are promising candidate because of small extent of electronic wavefunction (about 1 lattice constant).

- Substantial evidence of strong electron-phonon interaction (EPI) in oxides (manganite) using EXAFS.
- Qubits, based on oxide DQDs, hold promise in terms of coherence and miniaturization.
- In light-harvesting complexes highly efficient excitonic energy transfer takes place. Long-range FCN model is studied in this context [ Y-C. Cheng and G. R. Fleming, Annu. Rev. Phys. Chem. **60**, 241 (2009)].

# Thank you

Including the effect of small  $J_{\perp} e^{-g^2} / \omega$ :

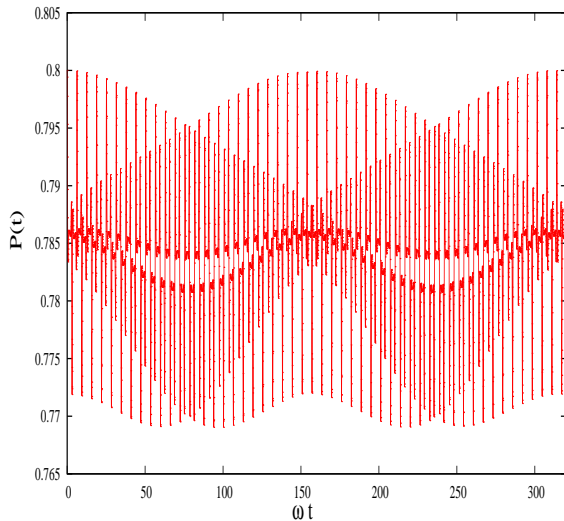


**Figure:** Time variation of the population difference  $P_d(t)$  for  $g = 2$  and  $J_{\perp} e^{-g^2} / \omega = 0.02$ . Figure correspond to the initial population difference  $[P_d(0)]$  value 0.8.

Including large number of bath modes ( $0.9\omega_u \leq \omega_k \leq \omega_u$ ):

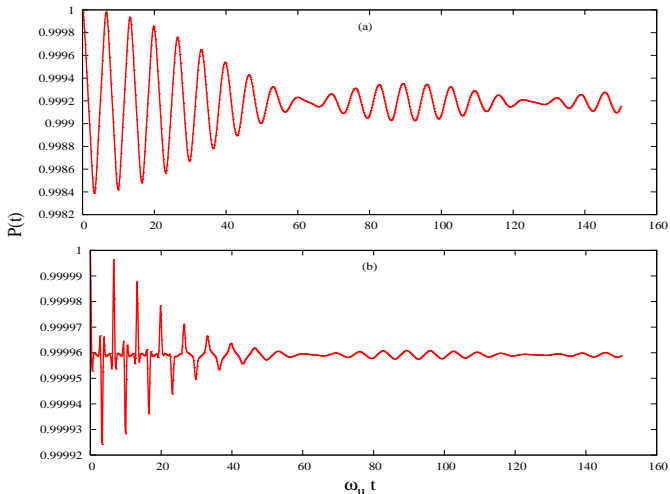


Figure: (a)  $J_{\perp}/\omega_u = 0.05$  and  $\frac{\sum_k g_k^2}{N} = 1$ ; (b)  $J_{\perp}/\omega_u = 0.05$  and  $\frac{\sum_k g_k^2}{N} = 4$ .

# Quantum control

- Due to the system-environmental coupling, the environment can distinguish among different states of the system. Thus different states acquire random relative phases and the reduced system faces decoherence.
- Quantum Zeno effect [QZE] is the arresting of decoherence in a quantum system through continuous measurements [B. Misra and E. C. G. Sudarshan, J. Math. Phys. **18**, 756 (1977)].

## Strategy for protection:

The system is perturbed much faster than the environment response time; the environment can not follow the change of system states anymore. So, the system is effectively decoupled from the environmental fluctuations.

Driving pulse:  $P_{\pi} = S_1^+ S_2^- + S_2^+ S_1^- \Rightarrow$  flips both the spins simultaneously.

Composite evolution operator:

$$U_1 = \tilde{U}(t + 2\delta t, t + \delta t)P_\pi \tilde{U}(t + \delta t, t)P_\pi$$

where

$$\begin{aligned}\tilde{U}(t, t') &= \tilde{U}(t, 0)\tilde{U}^\dagger(t', 0) = e^{iH_0 t} e^{-iHt} e^{iHt'} e^{-iH_0 t'} \\ &= e^{iH_0 t} e^{-iH(t-t')} e^{-iH_0 t'}.\end{aligned}$$

Now,

$$P_\pi e^{-i(H_0+H_I)\delta t} = e^{-i(H_0-H_I)\delta t} P_\pi$$

$\Rightarrow P_\pi$  pulse changes the sign of interaction. Thus applying  $P_\pi$  rapidly, produces decoupling from the environment.

$$\begin{aligned}U_1 &= \tilde{U}(t + 2\delta t, t + \delta t)P_\pi \tilde{U}(t + \delta t, t)P_\pi \\ &= I + O(\delta t^2)\end{aligned}$$

**If  $\delta t$  is small enough, evolution is almost unitary.**

PHYSICAL REVIEW B 89, 064311 (2014), A. Dey and Sudhakar Yarlagadda.

$N$  equispaced pulses (i.e.,  $\delta t = \frac{t}{N}$ ) yields:

$$\tilde{\rho}_T(t) = \left[ I + O[(\delta t)^2] \right]^{\frac{N}{2}} \rho_T(0) \left[ I + O[(\delta t)^2] \right]^{\frac{N}{2}}$$

$$\lim_{N \rightarrow \infty} \rho_s(t) = e^{-iH_s t} \rho_s(0) e^{iH_s t}.$$

Error:  $O[N(\delta t^2)] \sim O[(\delta t)]$  very small for  $\lim_{N \rightarrow \infty}$ .

Decoupling up to second order in  $\delta t$ :

$$e^{-i(H_0+H_I)\delta t} \approx e^{-iH_0\delta t} e^{-iH_I\delta t} e^{\frac{1}{2}[H_0, H_I]\delta t^2} + O(\delta t^3)$$

$$\begin{aligned} U_2 &= U_1 P_\pi U_1 P_\pi \\ &= \tilde{U}(t+4\delta t, t+3\delta t) P_\pi \tilde{U}(t+3\delta t, t+2\delta t) \tilde{U}(t+2\delta t, t+\delta t) P_\pi \tilde{U}(t+\delta t, t) \\ &= I + O[\delta t^3] \end{aligned}$$

$\Rightarrow$  Composite operator with unequally spaced pulses at  $\delta t$  and  $3\delta t$ .

Actually, ignoring terms of order  $\delta t^4$  and higher:

$$\begin{aligned} \langle \varepsilon_s | \rho_s(t) | \varepsilon_t \rangle &= \langle \varepsilon_s | \rho_s(0) | \varepsilon_t \rangle e^{-i(\varepsilon_s - \varepsilon_t)t} e^{\frac{i}{3}(J_\perp g^2 \omega^2 t \delta t^2)}, \\ \langle \varepsilon_s | \rho_s(t) | \varepsilon_s \rangle &= \langle \varepsilon_s | \rho_s(0) | \varepsilon_s \rangle. \end{aligned}$$

# Equilibrium value

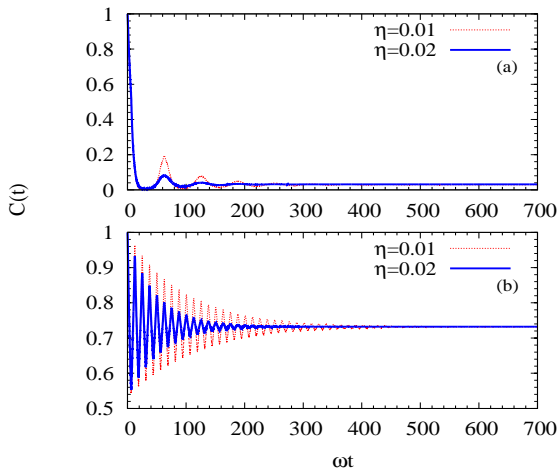


**Figure:** Time dependence of  $C(t)$  for  $\frac{J_{\perp}}{\omega} = 1.0$ ,  $g = 2.0$ , and when (a)  $\frac{\Delta\varepsilon}{\omega} = 7.9$  and (b)  $\frac{\Delta\varepsilon}{\omega} = 7.5$ .

# Global phonon coupling

$$H = H_s + H_B + H_I = H_s + \omega a^\dagger a + g\omega S_{\text{Total}}^z (a^\dagger + a)$$

$$\begin{aligned} & {}_s\langle \varepsilon | \rho_s^O(t) | \varepsilon' \rangle_s \\ &= \exp(-i [(\varepsilon - \varepsilon')t + \{(S_{T\varepsilon}^z)^2 - (S_{T\varepsilon'}^z)^2\} Y(t)]) \\ & \quad \times \exp[-(S_{T\varepsilon}^z - S_{T\varepsilon'}^z)^2 X(t)] {}_s\langle \varepsilon | \rho_s^O(0) | \varepsilon' \rangle_s \end{aligned}$$

## Schematic of

$(Insul.)/(LaMnO_3)_N/(SrMnO_3)_N/(Insul.)$

heterostructure. Strong multiferroicity and giant magnetoelectric effect is predicted.

S. Yarlagadda, P. B. Littlewood, P. Majumdar, R. Pankaj (arXiv:1203.3283).

